Research Square

Preprints are preliminary reports that have not undergone peer review.
They should not be considered conclusive, used to inform clinical practice,
or referenced by the media as validated information.

Spatiotemporal Variation in Forest Intrinsic Water-Use Efficiency and Its Sensitivity to Rising Atmospheric CO_2 in China During 1961–2012

Kangyuan Hong
Suqian University
Yuxin Xia
Suqian University
Muyi Li
limuyi@squ.edu.cn

Suqian University
Feng Yue
Guangdong University of Technology
Zhangli Sun
Guangdong University of Technology
Lidong Zou
Shenzhen Polytechnic University

Research Article

Keywords: China, tree-ring δ¹³C records, intrinsic water-use efficiency, C□, dW/dC□, carbon–water relationships

Posted Date: November 6th, 2026

DOI: https://doi.org/10.21203/rs.3.rs-11307287/v1

License: This work is licensed under a Creative Commons Attribution 4.0 International License.
Read Full License

Additional Declarations: No competing interests reported.

Spatiotemporal Variation in Forest Intrinsic Water-Use Efficiency and Its Sensitivity to Rising Atmospheric CO_2 in China During 1961–2012

Kangyuan Hong[1], Yuxin Xia[1], Muyi Li[1*], Feng Yue[2], Zhangli Sun[3], Lidong Zou[4]

[1]School of Civil Engineering and Architecture, Suqian University, Suqian 223800, People's Republic of China

[2]School of Architecture and Urban Planning, Guangdong University of Technology, Guangzhou 510006, People's Republic of China

[3]State Key Laboratory of Geohazard Prevention and Geo-environment Protection, College of Earth and Planetary Sciences, Chengdu University of Technology, Chengdu 610059, People's Republic of China

[4]School of Artificial Intelligence, Shenzhen Polytechnic University, Shenzhen 518055, China

Kangyuan Hong and Yuxin Xia contributed equally to this work.

[*]Corresponding author: Muyi Li

E-mail: limuyi@squ.edu.cn

Acknowledgments

We gratefully acknowledge the researchers and institutions that compiled and made publicly available the tree-ring $\delta^{13}C$, climate, elevation, and climate-classification datasets used in this study.

Key Message Forest iWUE increased across China during 1961–2012, whereas multiple temporal analyses provided no evidence of a significant long-term decline in CO_2-response sensitivity.

Abstract Rising atmospheric CO_2 concentration (C_a) has altered terrestrial carbon–water exchange, yet long-term changes in forest responses to increasing C_a remain uncertain. Based on 34 tree-ring $\delta^{13}C$ records from forests across China, we reconstructed forest intrinsic water-use efficiency (iWUE) from

1961 to 2012 and assessed its sensitivity to changes in C_a (dW/dC_a). Forest iWUE increased significantly during 1961–2012, with the regional mean rising from 64.36 μmol mol^{-1} in 1961 to 84.03 μmol mol^{-1} in 2012 at a rate of 0.4366 μmol mol^{-1} yr^{-1} ($P < 0.001$). All records showed positive trends, and 33 exhibited significant increases ($P < 0.05$). Despite increasing iWUE, dW/dC_a showed no significant long-term decline, with no significant temporal changes detected by moving-window analyses. Mean dW/dC_a was numerically lower during 2000–2012 (0.237 μmol mol^{-1} ppm^{-1}) than during 1961–1999 (0.305 μmol mol^{-1} ppm^{-1}), but the difference was not significant ($P = 0.509$). Spatial variation in dW/dC_a was not significantly associated with Köppen–Geiger climate regions. Environmental analyses identified MAP, MAT, and VP as relatively important factors, but their explanatory power was limited. These findings indicate that Chinese forests have increased iWUE under rising C_a without a detectable long-term decline in C_a response sensitivity.

Keywords: China; tree-ring $\delta^{13}C$ records; intrinsic water-use efficiency; C_a; dW/dC_a; carbon–water relationships

1 Introduction

Human activities have led to a rapid increase in atmospheric CO_2 concentration (C_a), profoundly altering terrestrial ecosystems and their interactions with global carbon and water cycles (Pan et al. 2011). Forests play a critical role in carbon sequestration and water use under climate change. In response to rising C_a and changing environmental conditions, plants can adjust carbon assimilation and stomatal regulation, thereby altering the balance between carbon gain and water loss (Zhang et al. 2023).

Intrinsic water-use efficiency (iWUE), defined as the ratio of photosynthetic carbon assimilation rate to stomatal conductance, is an important indicator of the trade-off between carbon assimilation and water use and of plant responses to environmental change (Medrano et al. 2009). The theoretical basis

of iWUE is closely linked to carbon isotope fractionation in plant leaves, through which the relationships among carbon assimilation, intercellular CO_2 concentration (C_i), and stomatal regulation can be characterized (Farquhar et al. 1989). Stable carbon isotope composition is closely related to the C_i/C_a ratio and stomatal regulation, providing a physiological basis for estimating iWUE from tree-ring $\delta^{13}C$ records (Pons and Helle 2011). Changes in iWUE integrate plant physiological responses to atmospheric C_a and hydroclimatic conditions, providing an indicator of long-term forest responses to environmental change (Battipaglia et al. 2013).

Tree-ring carbon isotope ($\delta^{13}C$) composition provides an effective means of reconstructing long-term variations in plant iWUE (Brienen et al. 2011; McCarroll and Loader 2004). Carbon isotope fractionation during photosynthesis is associated with stomatal conductance and carbon assimilation, allowing tree-ring $\delta^{13}C$ to record interannual physiological variations and long-term changes in iWUE (Rozendaal and Zuidema 2011). Studies in temperate forests of Europe and North America found that forest iWUE generally increased over the past century, commonly attributed to rising atmospheric C_a and associated changes in stomatal regulation (Saurer et al. 2004). Subsequent studies in Asia and other forest regions have shown that increasing iWUE is widespread under rising atmospheric C_a (Keenan et al. 2013).

However, increasing iWUE does not necessarily indicate unchanged forest responses to atmospheric C_a. A global synthesis showed that although forest iWUE has generally increased, its sensitivity to rising C_a (dW/dC_a) varies substantially among regions and has declined in some ecosystems (Adams et al. 2020). Thus, long-term iWUE trends alone may not fully capture forest responses to increasing C_a, highlighting the need to examine spatiotemporal variation in C_a-response sensitivity under different environmental conditions.

Whether these global patterns apply to regional forest ecosystems remains unclear. China provides

67 an appropriate setting because its forests span a broad climatic gradient, from humid subtropical forests
68 in the southeast to water-limited ecosystems in the northwest, encompassing diverse forest types and
69 physiological adaptation strategies (Han et al. 2023). Chinese forests have also experienced substantial
70 environmental changes in recent decades, including increasing atmospheric C_a and pronounced climatic
71 variability.

72 Previous tree-ring $\delta^{13}C$ studies have documented long-term variations in forest iWUE in humid
73 subtropical China (Li et al. 2017), arid and semi-arid northwestern China (Wang et al. 2012), and
74 temperate regions (Fu et al. 2020). However, these studies have largely focused on individual species or
75 local scales, limiting broader assessments across China. In particular, temporal variation in dW/dC_a, its
76 consistency across climatic regions, and its relationships with environmental factors remain insufficiently
77 characterized. Integrating tree-ring carbon isotope records across regions and multiple sequences can
78 therefore provide a regional-scale assessment of forest iWUE and its sensitivity to rising C_a.

79 In this study, we integrated 34 tree-ring carbon isotope records from different regions of China to
80 assess long-term variations in forest iWUE and its response to rising C_a. Specifically, the objectives were
81 to: (1) evaluate the long-term trend and spatial variation in forest iWUE in China during 1961–2012; (2)
82 determine whether dW/dC_a has changed over recent decades; and (3) investigate the associations of
83 climatic, topographic, and C_a background factors with spatial variation in dW/dC_a and assess their
84 relative contributions. We hypothesized that forest iWUE in China has generally increased over recent
85 decades, whereas its sensitivity to rising C_a may have changed over time in response to environmental
86 changes, plant physiological regulation, and climatic variability.

2 Research Data and Methods

2.1 Study Area and Isotope Dataset

The data used in this study were obtained from the global tree-ring stable carbon isotope ($\delta^{13}C$) dataset compiled by Adams et al. (2020) in their study, Diminishing CO_2-driven gains in water-use efficiency of global forests. This dataset integrates published tree-ring $\delta^{13}C$ records from sites worldwide and includes basic information such as site geographic coordinates, tree species, sampling periods, and annual tree-ring $\delta^{13}C$ series. It provides a fundamental dataset for investigating forest intrinsic water-use efficiency (iWUE) and its environmental responses under global change.

Based on this global tree-ring $\delta^{13}C$ dataset, we selected forest sampling sites located within mainland China according to their geographic coordinates and defined 1961–2012 as the study period. After screening, 34 valid tree-ring $\delta^{13}C$ records from Chinese forests were obtained, representing 32 sampling sites. Because some sampling sites contained multiple tree-ring sequences, individual tree-ring sequences were used as the basic units of analysis, while sampling-site effects were considered in analyses involving spatially replicated observations. The selected tree-ring sequences were distributed across forest regions with different geographical and environmental settings in China, forming a tree-ring network covering parts of the country's forested areas. This dataset provides a basis for examining spatial differences in forest iWUE and its sensitivity to changes in atmospheric CO_2 concentration (C_a) under different environmental conditions.

2.2 Reconstruction of iWUE and Calculation of Its Sensitivity to Changes in C_a

Based on the carbon isotope fractionation theory proposed by Farquhar et al., we reconstructed the annual iWUE of each tree-ring $\delta^{13}C$ sequence for 1961–2012 using the corresponding tree-ring $\delta^{13}C$

records. The atmospheric CO_2 concentration (C_a) data used in this study were consistent with those in the global tree-ring $\delta^{13}C$ database of Adams et al. (2020), ensuring consistent atmospheric CO_2 conditions for iWUE estimation across different tree-ring $\delta^{13}C$ records.

First, we calculated carbon isotope discrimination (Δ) from atmospheric CO_2 and tree-ring $\delta^{13}C$ values as follows:

$$\Delta = \frac{\delta^{13}C_a - \delta^{13}C_p}{1 + \delta^{13}C_p/1000}$$

where $\delta^{13}C_a$ represents the stable carbon isotope composition of atmospheric CO_2, and $\delta^{13}C_p$ represents the tree-ring $\delta^{13}C$ value.

We then calculated the ratio of intercellular to atmospheric CO_2 concentration (C_i/C_a) from the relationship between carbon isotope discrimination and intercellular CO_2 concentration:

$$\frac{C_i}{C_a} = \frac{\Delta - a}{b - a}$$

where a is the isotopic fractionation coefficient associated with the diffusion of CO_2 through stomata (4.4‰), and b is the isotopic fractionation coefficient associated with CO_2 fixation by Rubisco (27‰).

We calculated intrinsic water-use efficiency (iWUE, hereafter denoted as W) using the following equation:

$$W = \frac{C_a - C_i}{1.6}$$

that is,

$$W = \frac{C_a(1 - C_i/C_a)}{1.6}$$

where C_a is the atmospheric CO_2 concentration, C_i is the intercellular CO_2 concentration, and 1.6 represents the ratio of the diffusivities of CO_2 and water vapor during stomatal diffusion. This isotope-based approach has also been applied to tree-ring $\delta^{13}C$ records to estimate long-term variation in intrinsic water-use efficiency (Gentilesca et al. 2021).

To quantify the sensitivity of different forest ecosystems to changes in atmospheric CO_2 concentration, we further calculated the response slope of iWUE to changes in C_a (dW/dC_a). For each tree-ring $\delta^{13}C$ sequence, we estimated the response slope using ordinary least-squares (OLS) linear regression between annual iWUE and corresponding C_a values for 1961–2012:

$$W = a + bC_a$$

where b denotes dW/dC_a and represents the increase in iWUE per unit increase in C_a. A higher dW/dC_a indicates greater sensitivity of the forest ecosystem's iWUE to changes in C_a. We estimated dW/dC_a for each tree-ring $\delta^{13}C$ sequence using all available valid-year observations and recorded the coefficient of determination (R^2) and P value for each regression to evaluate the fit of the response relationship.

2.3 Environmental Data

2.3.1 Climate Variables

Annual mean temperature (MAT), annual mean precipitation (MAP), vapor pressure (VP), and potential evapotranspiration (PET) were selected as the primary climate variables in this study.

The climate data were obtained from the Climatic Research Unit (CRU) TS v4.09 global climate dataset released by the Climatic Research Unit at the University of East Anglia, UK (Harris et al. 2020). The data can be downloaded from the CRU TS v4.09 website. The dataset provides monthly climate data for global terrestrial areas at a spatial resolution of 0.5° × 0.5°. We extracted annual climate data for 1961–2012 and, based on the geographic coordinates of the tree-ring $\delta^{13}C$ records, extracted the corresponding MAT, MAP, VP, and PET values at each location using spatial matching.

For each tree-ring $\delta^{13}C$ sequence, the annual climate data for 1961–2012 were averaged over the study period to obtain the long-term mean climatic conditions associated with each sequence. These long-

term mean climate variables were used as environmental explanatory variables and matched with the corresponding dW/dC_a values calculated for each tree-ring $\delta^{13}C$ sequence to examine spatial differences in forest sensitivity to changes in C_a under different environmental conditions and its associations with environmental factors. In addition, PET and MAP were used to calculate the Aridity Index (AI) to characterize the long-term water availability relative to atmospheric water demand experienced by each tree-ring $\delta^{13}C$ sequence.

2.3.2 Aridity Index

To further characterize the degree of water limitation experienced by the tree-ring $\delta^{13}C$ records, the Aridity Index (AI) was calculated as follows (Zomer et al. 2022):

$$AI = \frac{MAP}{PET}$$

where MAP represents mean annual precipitation and PET represents potential evapotranspiration. The AI integrates the long-term balance between regional water input and potential atmospheric water demand. Lower AI values indicate that precipitation supply is relatively insufficient compared with evaporative demand, corresponding to greater regional water deficits and more arid climatic conditions.

It should be noted that AI and VP characterize different aspects and dimensions of the moisture environment. AI is primarily used to characterize the long-term regional balance between water supply and atmospheric water demand, thereby reflecting the overall moisture regime of the ecosystem. In contrast, VP represents atmospheric moisture conditions. Thus, AI and VP characterize regional water availability and atmospheric moisture status, respectively.

Long-term water limitation may alter stomatal regulation and CO_2 diffusion into leaves, thereby affecting iWUE and its sensitivity to changes in C_a (dW/dC_a). Therefore, AI was used to characterize different moisture conditions and to further examine differences in the responses of forest vegetation in

China to increasing C_a under different moisture regimes.

2.3.3 Digital Elevation Model (DEM)

We used the Shuttle Radar Topography Mission (SRTM) V3.0 global digital elevation model (DEM) dataset (Farr et al. 2007) (USGS/SRTMGL1_003) to represent topographic variation across the study region at a spatial resolution of approximately 30 m. The DEM data were obtained through the Google Earth Engine (GEE) platform and clipped to the extent of China before download. Because of the large spatial extent of the study area, the downloaded data consisted of 20 GeoTIFF raster tiles. We mosaicked these DEM tiles in QGIS and standardized the coordinate reference system to WGS 84. We extracted elevation values (m) at the geographic coordinates of the tree-ring $\delta^{13}C$ records and used elevation as a predictor of spatial variation in dW/dC_a.

2.3.4 Köppen–Geiger Climate Classification

We used the Köppen–Geiger climate classification system to examine variations in forest iWUE and C_a-response sensitivity across different climatic settings in China.

We obtained the Köppen–Geiger climate classification dataset developed from the Figshare platform (https://doi.org/10.6084/m9.figshare.6396959) (Beck et al. 2018). We used the current climate version (V1) at a spatial resolution of 0.5°. We assigned each tree-ring $\delta^{13}C$ sequence to the corresponding Köppen–Geiger climate type based on its geographic coordinates.

Based on the Köppen–Geiger climate types assigned to the tree-ring $\delta^{13}C$ records, the 34 forest tree-ring $\delta^{13}C$ records were classified into different climate groups. The sequences were mainly distributed across arid (B), temperate (C), and continental (D) climate regions in China, with no sequences located in tropical (A) or polar (E) climate regions. Therefore, the 34 forest tree-ring $\delta^{13}C$ records were ultimately classified into three major climate groups: B, C, and D. The trends and magnitudes of changes in forest

iWUE, as well as differences in sensitivity to increasing C_a (dW/dC_a), were then compared among these climatic settings.

2.4 Statistical Analysis

2.4.1 Analysis of Long-Term Trends in iWUE

To assess the long-term trend in forest iWUE in China during 1961–2012, we calculated the annual mean iWUE across all available tree-ring sequences and used the standard error (SE) to quantify its uncertainty. We fitted an ordinary least-squares (OLS) linear regression to the annual mean iWUE and used the regression slope to quantify its rate of change over the study period. We assessed the statistical significance of the trend using the non-parametric Mann–Kendall (MK) test (Mann 1945) at $\alpha = 0.05$. Because the MK test does not require normally distributed data and is relatively robust to outliers, we used it to test whether the iWUE time series showed a significant monotonic trend. We also calculated the coefficient of determination (R^2) from the OLS regression to quantify the goodness of fit of the linear trend. We used the OLS regression slope to quantify the long-term rate of change, the MK P value to assess trend significance, and R^2 as an auxiliary measure of the linear fit.

2.4.2 Temporal Evolution of C_a-Response Sensitivity

We used C_a-response sensitivity (dW/dC_a) to quantify the change in forest iWUE per unit change in C_a. We used this metric to compare C_a-response sensitivity across different periods and environmental conditions. We estimated dW/dC_a at both the tree-ring $\delta^{13}C$ sequence level and the regional level.

At the sequence level, each tree-ring $\delta^{13}C$ sequence was treated as an independent analytical unit. For each tree-ring $\delta^{13}C$ sequence, we fitted a simple linear regression between annual iWUE and corresponding C_a values for 1961–2012 and used the regression slope as the dW/dC_a estimate. We used sequence-level dW/dC_a estimates to examine their spatial variation and relationships with climatic

variables, including MAT, MAP, VP, PET, and AI.

At the regional level, we calculated the annual mean iWUE across the 34 tree-ring $\delta^{13}C$ records to obtain a regional iWUE time series for China. We then fitted a linear regression between regional mean iWUE and C_a and used the regression slope to estimate regional-scale dW/dC_a. We used regional-scale dW/dC_a to examine the long-term temporal variation in forest C_a-response sensitivity during 1961–2012.

To further examine temporal variation in dW/dC_a, we applied a moving-window analysis. We used 5-, 10-, and 20-year moving windows. Within each window, we fitted a simple linear regression between annual iWUE and C_a and used the regression slope as the dW/dC_a estimate for that period. We shifted the window forward by one year at a time to generate a continuous dW/dC_a time series.

We selected the 5-, 10-, and 20-year windows to assess the consistency of dW/dC_a variation across temporal scales. The 5-year window captured short-term fluctuations in iWUE responses to changes in C_a; the 10-year window was used as the primary analysis window because it reduces interannual variability while retaining decadal-scale information; and the 20-year window captured smoother changes in dW/dC_a over longer timescales. We compared the direction of dW/dC_a changes across window lengths to assess the sensitivity of the results to temporal scale.

Considering that short time windows may reduce the degrees of freedom for regression and increase uncertainty in dW/dC_a estimates, we required each 5-, 10-, and 20-year window to contain complete consecutive annual observations. We retained only windows without missing years for regression analysis.

2.4.3 Climate Comparison Analysis

We assigned the sampling locations of the tree-ring sequences to Köppen–Geiger climate zones and compared dW/dC_a among climate regions. Based on the climate types at the sampling locations, we

classified the sequences into arid (B), temperate (C), and continental (D) climate regions. We calculated the mean dW/dC_a and its 95% confidence interval for each climate region. Combined with the distribution of response sensitivity across individual tree-ring sequences, the spatial differences in forest sensitivity to changes in C_a under different climatic settings were further examined.

Considering that the 34 tree-ring $\delta^{13}C$ records in this study were obtained from 32 sampling sites, with some sites containing multiple tree-ring sequences, sequences from the same site may share similar climatic, ecological, and geographic conditions. We therefore fitted a linear mixed-effects model (LMM) to assess differences in dW/dC_a among Köppen–Geiger climate types. We treated Köppen–Geiger climate type as a fixed effect and sampling site as a random effect (Bates et al. 2015) to account for potential non-independence among observations when multiple tree-ring sequences originated from the same sampling site. We assessed the significance of climate-type differences using the P value for the fixed effect.

2.4.4 Random Forest and SHAP Interpretability Analysis

To explore the relative contributions of environmental factors to spatial variation in dW/dC_a and their potential nonlinear associations, we combined a Random Forest (RF) model with SHAP (SHapley Additive exPlanations) analysis (Breiman 2001). Given the limited sample size, we did not use the RF model as a predictive model. Instead, we used it as an exploratory tool to assess the relative importance of environmental factors and their potential nonlinear associations with dW/dC_a.

We used dW/dC_a estimates from the 34 tree-ring $\delta^{13}C$ records as the response variable and included MAT, MAP, VP, AI, elevation (DEM), latitude (Lat), longitude (Lon), and C_a as candidate predictors. We checked all variables for missing values before analysis and used the resulting complete dataset for model fitting. We configured the Random Forest model with 200 decision trees, a minimum leaf size of 3

samples, and all predictor variables considered at each node split. We set the random seed to 42 to ensure reproducibility.

Given the small sample size (n = 34), we used leave-one-out cross-validation (LOOCV) to evaluate out-of-sample model performance (Stone 1974), using the coefficient of determination (R^2) and root mean square error (RMSE) as performance metrics. We also compared the relative importance of environmental factors using out-of-bag (OOB) permutation importance from the RF model fitted to the full dataset.

Furthermore, SHAP was used to interpret the Random Forest results. SHAP values were calculated for each environmental factor to quantify the marginal contribution and direction of different variable values to the model predictions of dW/dC_a. A SHAP summary plot was used to compare the relative importance of environmental factors, while SHAP dependence plots were used to examine the response direction and potential nonlinear relationships between key environmental factors and the model-predicted dW/dC_a.

3 Results

3.1 Dataset Overview

We compiled 34 tree-ring $\delta^{13}C$ records from China covering 1961–2012 to examine long-term variation in forest iWUE and C_a-response sensitivity (dW/dC_a). The 34 tree-ring $\delta^{13}C$ records were obtained from 32 sampling sites and were distributed approximately between 73° E – 135° E and 5° N – 53° N, covering parts of the forested regions of China. According to the Köppen–Geiger climate classification system, the sequences were mainly distributed across arid (B), temperate (C), and continental (D) climate regions, with relatively more tree-ring sequences located in the C and D climate regions (Fig. 1a).

The 34 sequences all contained valid observations within the 1961–2012 study period, but their temporal coverage and record lengths varied substantially (Fig. 1b). The valid record length of individual sequences ranged from 7 to 52 years. Some sequences covered the entire study period, whereas others contained observations for only part of the study period. The number of valid tree-ring $\delta^{13}C$ records remained within a relatively narrow range during 1961–2012, although some interannual variation occurred (Fig. 1c). Overall, the dataset covered diverse climatic settings in China and included tree-ring $\delta^{13}C$ records of varying lengths, allowing us to assess long-term changes in iWUE and its response to C_a.

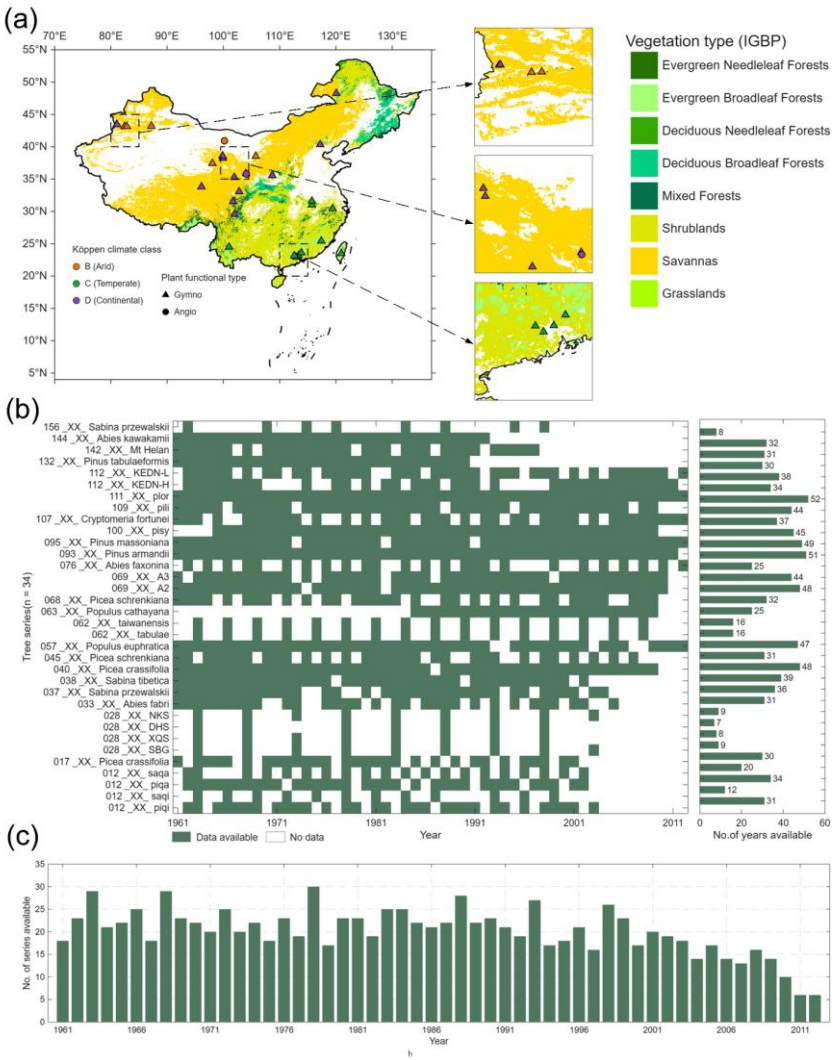


Fig. 1 Spatial distribution and temporal coverage of the 34 tree-ring $\delta^{13}C$ records in China

(a) Spatial distribution of sampling locations and climate types. The background represents global vegetation types

based on the IGBP classification. Colors indicate Köppen–Geiger climate types: orange, green, and purple represent B (arid), C (temperate), and D (continental) climate types, respectively. Different symbols indicate plant functional groups, with triangles representing gymnosperms and circles representing angiosperms. The enlarged panels show sampling locations in northwestern, northern, and southern China.

(b) Temporal coverage of the 34 tree-ring $\delta^{13}C$ records during 1961–2012. Dark green indicates years with valid observations, blank areas indicate missing data, and bars represent the number of valid years for each record.

(c) Annual variation in the number of tree-ring $\delta^{13}C$ records with valid observations during 1961–2012.

3.2 Long-Term Temporal Trend in iWUE

From 1961 to 2012, forest iWUE in China exhibited a significant long-term increasing trend (Fig. 2a). The regional mean iWUE reconstructed from the 34 tree-ring $\delta^{13}C$ records increased from 64.36 μmol mol^{-1} in 1961 to 84.03 μmol mol^{-1} in 2012, representing a cumulative increase of approximately 31%. Forest iWUE increased significantly at a rate of 0.4366 μmol mol^{-1} yr^{-1} during the study period (R^2 = 0.89), and the Mann–Kendall (MK) test also indicated a significant increasing trend ($P < 0.001$), indicating a sustained increase in forest ecosystem iWUE in China over the past half-century (Fig. 2a). Sequence-level trend analysis further showed that all 34 tree-ring isotope sequences exhibited positive trends, with 33 sequences showing statistically significant increases ($P < 0.05$). The spatial distribution of these interannual iWUE trends is shown in Online Resource 1 (Fig. S3). Because record lengths varied substantially among sequences, sequence-level trends should be interpreted with caution. Overall, the consistency in the direction of change across sequences supports the long-term increasing trend in forest iWUE across the study region (Online Resource 1, Fig. S1).

The multi-year mean iWUE showed pronounced spatial heterogeneity across the 34 tree-ring $\delta^{13}C$ records (Fig. 2b). The distribution of iWUE across the Köppen–Geiger climate types is further shown

in Online Resource 1 (Fig. S2). The mean iWUE of individual tree-ring $\delta^{13}C$ records ranged approximately from 50 to 100 μmol mol^{-1}. Relatively high mean iWUE values occurred mainly in sequences from inland northwestern and northeastern China, whereas some sequences in the humid eastern regions exhibited relatively lower iWUE levels. These differences indicate substantial spatial variation in forest iWUE across China. Overall, forest iWUE in China exhibited a significant increasing trend from 1961 to 2012, together with pronounced spatial heterogeneity. Additional Pearson and partial correlation analyses between iWUE and major climatic factors across the different Köppen–Geiger climate regions are provided in Online Resource 1 (Figs. S4 and S5).

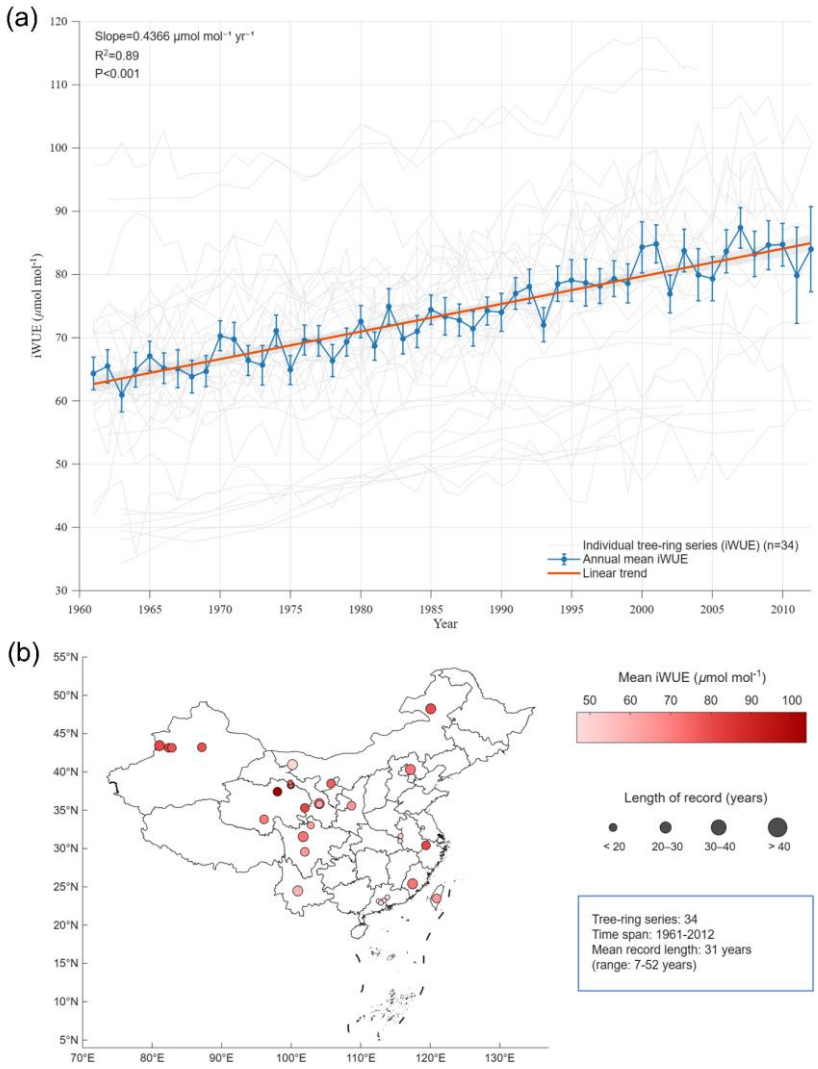


Fig. 2 Long-term temporal trend and spatial pattern of forest iWUE in China during 1961–2012

(a) Annual variation in regional mean iWUE. Gray thin lines represent individual tree-ring $\delta^{13}C$ records, blue circles and error bars indicate annual mean iWUE and standard error (SE), respectively, and the red line shows the linear trend.

(b) Spatial distribution of multi-year mean iWUE. Circle color indicates mean iWUE, and circle size represents the valid record length of each tree-ring $\delta^{13}C$ record.

3.3 Long-Term Variation in C_a-Response Sensitivity (dW/dC_a)

Forest iWUE generally increased with C_a during 1961–2012, but the magnitude of the increase per unit change in C_a varied over time (Fig. 3). Across the entire study period, iWUE showed a strong quadratic relationship with C_a ($R^2 = 0.89$, $P < 0.001$). The fitted curve indicated an overall increase in forest iWUE with increasing C_a, while the iWUE gain per unit increase in C_a gradually decreased (Fig. 3a). Separate linear regressions were fitted for the two predefined periods (1961–1999 and 2000–2012) to compare the magnitude of iWUE change per unit increase in C_a between periods.

Further analysis divided the study period into two stages, 1961–1999 and 2000–2012, to compare changes in the sensitivity of forests to increasing C_a between the two periods (Fig. 3b). Because some tree-ring sequences did not extend to 2012, 17 sequences that covered both 1961–1999 and 2000–2012 were selected for paired analysis to ensure that the comparison between the two periods was based on the same tree-ring sequences. The dW/dC_a value for each sequence was calculated separately for the two periods, and changes in sequence-level response sensitivity were compared. The results showed that the mean dW/dC_a was 0.305 and 0.237 $\mu mol\ mol^{-1}\ ppm^{-1}$ during 1961–1999 and 2000–2012, respectively. Although the mean response sensitivity was lower during the later period than during the earlier period, the paired t-test indicated that the difference between the two periods was not statistically significant ($P = 0.509$).

To further evaluate the timescale dependence of changes in dW/dC_a, sensitivity analyses were conducted using 5-, 10-, and 20-year moving windows (Fig. 3c–e). The slopes of dW/dC_a changes were close to zero across all window lengths, and no clear long-term decreasing trend was observed. The linear slopes for the 5-, 10-, and 20-year windows were −0.005 (R^2 = 0.015, P = 0.401), −0.002 (R^2 = 0.025, P = 0.309), and 0.001 (R^2 = 0.098, P = 0.076), respectively.

At the decadal scale, the study period was divided into five stages: 1961–1970, 1971–1980, 1981–1990, 1991–2000, and 2001–2010, to examine the variation in dW/dC_a (Fig. 3f). No significant differences in response sensitivity were detected among the five periods (P = 0.610).

Overall, forest iWUE in China continued to increase with increasing C_a during 1961–2012, and the fitted relationship indicated a decreasing iWUE gain per unit increase in C_a. However, neither the comparison between periods based on the 17 common sequences, nor the sensitivity analyses across different temporal scales or the decadal comparison detected a statistically significant long-term decline in dW/dC_a.

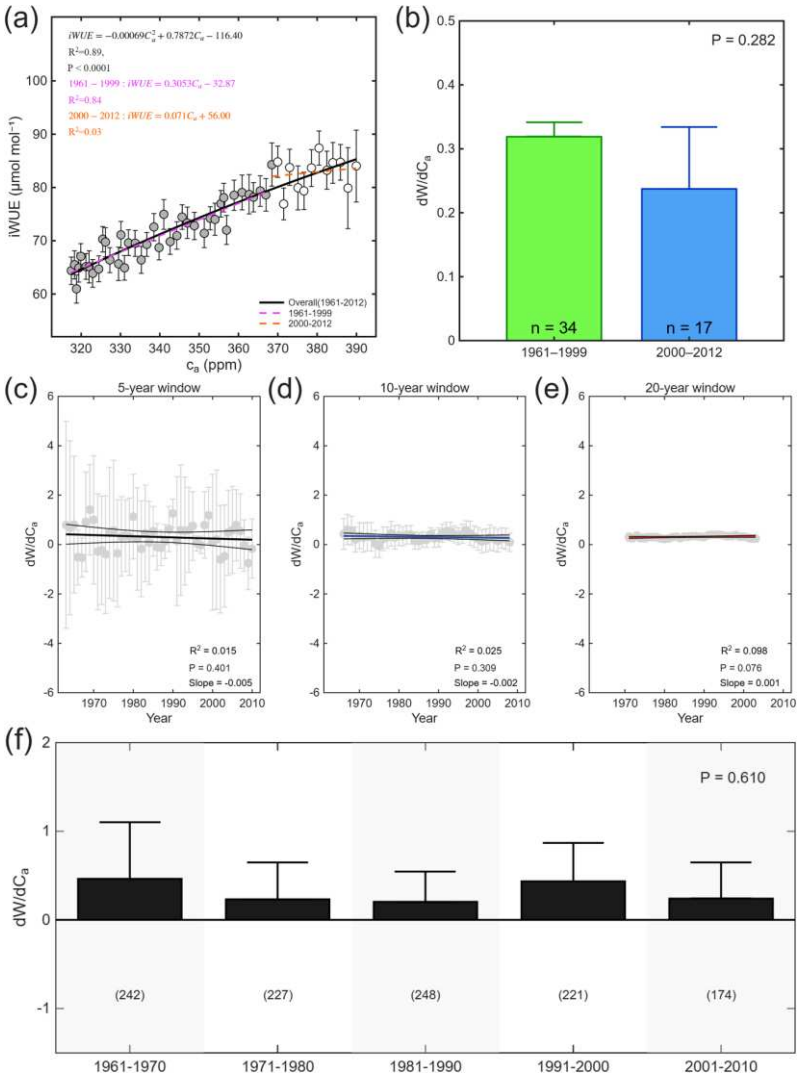


Fig. 3 Temporal variation in the sensitivity of forest iWUE to increasing C_a (dW/dC_a) in China

(a) Fitted relationships between iWUE and C_a for the full period (1961–2012) and two subperiods (1961–1999 and 2000–2012). Points represent annual regional mean iWUE, and vertical error bars represent the standard deviation (SD) of iWUE. The black solid line represents the quadratic fit for the full period (1961–2012), the purple dashed line represents the linear fit for 1961–1999, and the orange dashed line represents the linear fit for 2000–2012. The fitted equations, coefficients of determination (R^2), and significance P values for each period are shown in the upper-left corner

(b) Comparison of dW/dC_a between different periods. Mean dW/dC_a values for the two periods were calculated from the 17 tree-ring sequences that simultaneously covered 1961–1999 and 2000–2012. Error bars represent the standard

error (SE), and the P value indicates the result of the paired t-test

(c–e) Annual variation in dW/dC_a estimated using 5-, 10-, and 20-year moving windows, respectively, to test the robustness of the dW/dC_a trend to the choice of window length. Light gray points represent dW/dC_a values estimated for each moving window, and gray error bars represent the 95% confidence intervals of the corresponding slopes. Solid lines represent the linear trends in dW/dC_a for each window length. The trend slope, R^2, and P value are indicated in each panel

(f) Mean dW/dC_a and its variation across successive 10-year periods from 1961 to 2010. Black bars represent the mean values for each period, and error bars represent the 95% confidence intervals of the regression slopes. Numbers in parentheses indicate the effective sample size for each period, and the P value in the upper-right corner indicates the result of the overall test for differences among the decadal periods

3.4 Spatial Differentiation in C_a-Response Sensitivity (dW/dC_a)

We compared dW/dC_a among the 34 tree-ring $\delta^{13}C$ records across Köppen–Geiger climate regions. The results showed that all 34 tree-ring isotope sequences had positive dW/dC_a values, with an overall mean dW/dC_a of approximately 0.34 μmol mol^{-1} ppm^{-1}. The 95% confidence interval is shown in Fig. 4a.

Mean dW/dC_a varied among the Köppen–Geiger climate zones. The arid climate region (B, n = 8) had a mean dW/dC_a of approximately 0.30 μmol mol^{-1} ppm^{-1}, with relatively large variation among sequences; the temperate climate region (C, n = 10) had a mean value of approximately 0.36 μmol mol^{-1} ppm^{-1}; and the continental climate region (D, n = 16) had a mean value of approximately 0.34 μmol mol^{-1} ppm^{-1}, with a relatively concentrated distribution. The dW/dC_a distributions overlapped among climate regions. The linear mixed-effects model detected no significant differences in dW/dC_a among climate regions (P = 0.489). Sensitivity analyses using one-way ANOVA and the Kruskal–Wallis test

yielded the same inference (Online Resource 1, Table S1).

Overall, all 34 tree-ring isotope sequences exhibited positive dW/dC_a values. Although the mean dW/dC_a differed to some extent among the different Köppen–Geiger climate regions, these differences did not reach statistical significance.

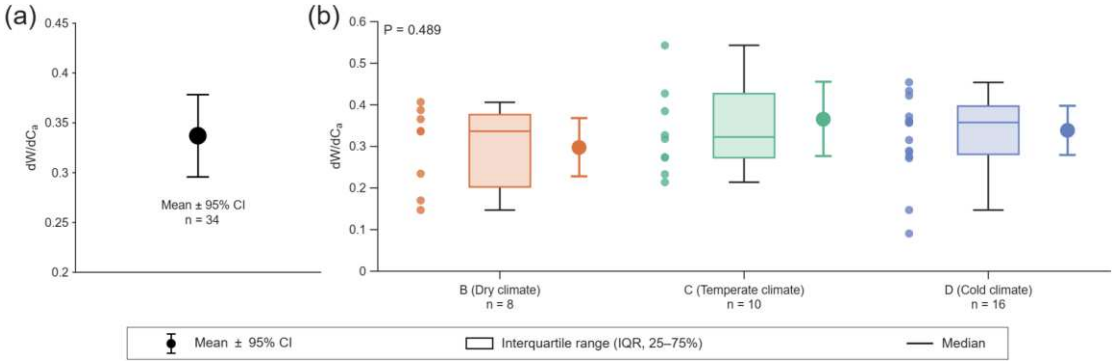


Fig. 4 Spatial differences in the sensitivity of forest iWUE to increasing C_a (dW/dC_a) across different Köppen–Geiger climate regions in China

(a) Overall mean dW/dC_a and its 95% confidence interval based on the dW/dC_a values of the 34 tree-ring $\delta^{13}C$ records. The black filled circle represents the overall mean dW/dC_a across the 34 tree-ring sequences, and the vertical black line represents its 95% confidence interval. The sample size is indicated as n = 34

(b) Distribution of dW/dC_a across Köppen–Geiger climate types. Arid (B, n = 8), temperate (C, n = 10), and continental (D, n = 16) climate regions indicate the numbers of tree-ring $\delta^{13}C$ records in each group. Colored points represent individual dW/dC_a values. Boxes show the interquartile range (IQR; 25th–75th percentiles), with the horizontal line indicating the median. Whiskers represent the minimum and maximum values excluding outliers. Large circles indicate mean dW/dC_a values, and error bars show 95% confidence intervals. Differences among climate types were evaluated using a linear mixed-effects model (LMM), with climate type as a fixed effect and sampling site as a random effect.

3.5 Associations Between Environmental Factors and Spatial Variation in dW/dC_a

We combined partial correlation, Random Forest, and SHAP analyses to examine associations between environmental factors and spatial variation in dW/dC_a (Fig. 5). Additional scatterplots and linear fits between dW/dC_a and the major environmental factors across the different Köppen–Geiger climate regions are provided in Online Resource 1 (Fig. S6).

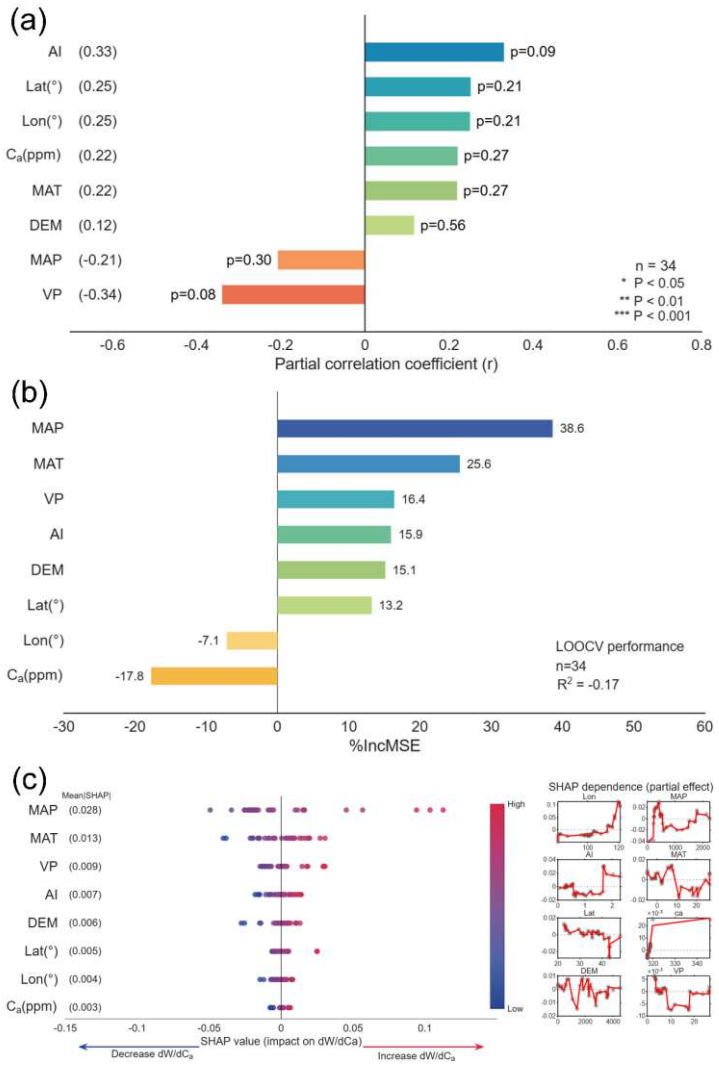
Partial correlations between environmental factors and dW/dC_a varied in magnitude (Fig. 5a). AI was positively correlated with dW/dC_a ($r = 0.33$), whereas VP showed a negative correlation ($r = -0.34$); however, neither correlation reached statistical significance ($P > 0.05$). MAT and C_a showed weak positive correlations with dW/dC_a ($r = 0.22$), whereas MAP showed a weak negative correlation ($r = -0.21$). Overall, no individual environmental factor showed a significant linear relationship with dW/dC_a, indicating that simple correlation analysis alone may not fully capture the combined effects of environmental factors on C_a-response sensitivity.

We further used the Random Forest model to assess the relative importance of environmental factors for spatial variation in dW/dC_a (Fig. 5b). The LOOCV results showed that the model had an R^2 of −0.17, indicating limited predictive performance for the spatial variation in dW/dC_a under the current sample size and combination of environmental variables. In the variable-importance analysis, MAP, MAT, and VP ranked relatively high in variable importance, with increases in mean squared error based on out-of-bag (OOB) permutation (%IncMSE) of 38.6%, 25.6%, and 16.4%, respectively, followed by AI (15.9%) and DEM (15.1%). Latitude and longitude showed relatively lower importance (13.2% and 7.1%, respectively), whereas C_a did not show high importance.

SHAP analysis further indicated that some environmental variables may exhibit nonlinear

associations with model-predicted dW/dC_a (Fig. 5c). The SHAP responses of MAP, MAT, and VP showed nonlinear patterns to some extent, suggesting potentially complex statistical associations between these variables and model-predicted dW/dC_a. Specifically, the SHAP responses of MAP, MAT, and VP all exhibited varying degrees of nonlinear variation, indicating that their associations with dW/dC_a differed across environmental gradients. In contrast, C_a, latitude, longitude, and DEM had relatively low mean absolute SHAP values, suggesting relatively limited contributions to the spatial variation in dW/dC_a.

Taken together, the results of the partial correlation, Random Forest, and SHAP analyses showed that MAP, MAT, and VP consistently ranked relatively high in importance across the different statistical analyses. Given the relatively low overall predictive performance of the Random Forest model (LOOCV $R^2 = -0.17$), the variable-importance results were primarily used to characterize the relative contributions of different environmental factors to the spatial variation in dW/dC_a. In contrast, C_a, latitude, longitude, and DEM showed relatively low contributions across multiple analyses.



445

446 Fig. 5 Associations between environmental factors and spatial variation in dW/dC_a of forests in

447 China

448 (a) Partial correlation analysis between environmental factors and dW/dC_a. Partial correlation coefficients (r) were

449 calculated after controlling for other environmental variables. Blue and orange indicate positive and negative

450 correlations, respectively. Values in parentheses represent correlation coefficients, and significance levels are

451 indicated at the ends of the bars ($P < 0.05$, $P < 0.01$, and $P < 0.001$). The analyzed variables included AI, Lat, Lon,

452 C_a, MAT, DEM, MAP, and VP ($n = 34$).

453 (b) Relative importance of environmental variables based on the Random Forest model. Variable importance was

454 quantified using out-of-bag permutation importance and expressed as the percentage increase in mean squared error

(%IncMSE). Larger values indicate greater contributions to model performance. Model performance based on leave-one-out cross-validation (LOOCV) is shown in the lower-right corner (n = 34, $R^2 = -0.17$).

(c) SHAP analysis of the associations between environmental factors and model-predicted dW/dC_a. Mean|SHAP| values indicate the relative importance of variables. Each point represents the SHAP contribution of an individual sample; positive and negative values indicate higher and lower predicted dW/dC_a values, respectively. Colors indicate the magnitude of each variable. SHAP dependence curves show nonlinear relationships between individual environmental variables and model predictions.

4 Discussion

4.1 Long-Term Increase in Forest iWUE in China and Its Global Consistency

Using 34 tree-ring $\delta^{13}C$ records, we reconstructed forest iWUE in China for 1961–2012 and assessed its long-term variation. The results showed a significant increasing trend in forest iWUE over the past half-century, with all 34 tree-ring sequences exhibiting positive trends and 33 reaching statistical significance. This finding is consistent with long-term studies based on tree-ring $\delta^{13}C$ at the global scale, indicating that forest ecosystems have generally undergone adjustments in the balance between carbon gain and water loss under continuously rising C_a (Ding et al. 2026). Chinese forests span a broad climatic gradient, from arid and semi-arid regions to humid forest regions. Despite substantial differences in environmental conditions among regions, the overall consistency in the direction of change suggests that continuously rising C_a may have been an important background factor contributing to adjustments in forest water-use strategies over recent decades.

According to the Farquhar theory of carbon isotope fractionation, changes in plant iWUE are primarily determined by the relative changes in intercellular CO_2 concentration (C_i) and C_a. As C_a has

continuously increased since industrialization, plants can maintain a certain level of carbon assimilation under lower stomatal opening, thereby increasing carbon gain per unit of water loss and increasing iWUE. The increase in forest iWUE may result from enhanced photosynthetic carbon assimilation, reduced stomatal conductance, or a combination of both, with their relative contributions varying with environmental conditions (Antonucci et al. 2023; Guerrieri et al. 2019). Previous global-scale tree-ring studies have shown that most forest ecosystems exhibited pronounced increases in iWUE during the latter half of the twentieth century, and the present study further indicates that this global response pattern also applies to forest ecosystems in China (Mathias and Thomas 2021).

However, the long-term increase in iWUE does not necessarily imply that all ecosystems respond to rising C_a in the same way (Peñuelas et al. 2011). Plant responses to changes in atmospheric CO_2 are jointly influenced by plant functional types, environmental conditions, and long-term physiological acclimation (Franks et al. 2013). In addition to changes in C_a, regional climatic conditions and plant physiological regulation may also affect the magnitude of changes in iWUE. Previous tree-ring studies have shown that variation in water availability can influence $\delta^{13}C$ and water-use efficiency, indicating that hydroclimatic conditions may contribute to differences in physiological responses among forest sites (Gebrekirstos et al. 2011). Persistent warming, changes in water availability, and variations in atmospheric dryness may alter stomatal regulation and carbon–water exchange processes, thereby contributing to differences in the magnitude of iWUE increases across forest regions. It should be noted, however, that this study primarily focused on iWUE and its responses to changes in C_a during 1961–2012 and did not directly disentangle the relative contributions of different environmental factors to long-term changes in iWUE. Therefore, the environmental effects discussed above should be regarded as potential mechanisms rather than direct causal attributions.

Although forest iWUE in China exhibited a sustained increasing trend, iWUE itself reflects the efficiency of carbon uptake per unit of stomatal water loss and therefore cannot directly represent total ecosystem-scale transpiration, changes in water consumption, or carbon sink capacity (Andreu-Hayles et al. 2011). Thus, an increase in iWUE alone is insufficient to fully characterize the response of forest ecosystems to continuously rising C_a. Further analysis of C_a-response sensitivity (dW/dC_a), defined as the magnitude of change in iWUE per unit increase in C_a, can provide additional insight into the marginal response of forests to continuously rising C_a.

4.2 Long-Term Changes and Regional Differences in C_a-Response Sensitivity

In contrast to the sustained increase in iWUE, forest C_a-response sensitivity (dW/dC_a) in China did not show a significant long-term decline, differing from the decline reported for some forest ecosystems at the global scale (Adams et al. 2020). Among the 17 tree-ring sequences that covered both 1961–1999 and 2000–2012, mean dW/dC_a was numerically lower in 2000–2012 (0.237 μmol mol^{-1} ppm^{-1}) than in 1961–1999 (0.305 μmol mol^{-1} ppm^{-1}), but the difference was not statistically significant based on the paired t-test ($P = 0.509$). Sensitivity analyses using 5-, 10-, and 20-year moving windows likewise showed no consistent declining pattern in dW/dC_a across window lengths. Therefore, within the temporal and sampling ranges examined here, we found no statistically significant evidence of a long-term decline in forest C_a-response sensitivity in China.

This distinction suggests that iWUE and dW/dC_a capture different aspects of forest responses to rising C_a. iWUE describes the level of carbon gain per unit of water loss by plants over a given period, whereas dW/dC_a reflects changes in the magnitude of iWUE gains as atmospheric C_a continues to increase. Thus, continued increases in iWUE do not necessarily imply a corresponding increase in the

521 marginal response to additional C_a. Incorporating dW/dC_a alongside long-term iWUE trends provides
522 additional insight into the magnitude and temporal variation of forest responses to rising C_a.

523 Recent global-scale studies have suggested that dW/dC_a may decline over time in some forest
524 ecosystems, potentially due to diminishing marginal effects of CO_2 fertilization, photosynthetic
525 acclimation, increasing nutrient limitation, and changes in hydroclimatic conditions (Ainsworth and
526 Long 2005; Knauer et al. 2017). However, this study did not detect a significant declining trend in
527 dW/dC_a across Chinese forests, which may be related to differences in the geographic extent, sample
528 composition, and temporal scales of the studies. The tree-ring sequences analyzed here mainly represent
529 temperate, cold, and arid climate regions, whereas global syntheses encompass a broader range of forest
530 types and environmental conditions. Differences in study periods, sample sizes, and tree-ring record
531 lengths may also influence estimates of dW/dC_a trends. Thus, our results do not show a significant decline
532 in dW/dC_a comparable to that reported for some global forest ecosystems.

533 Although this study did not detect a significant decline in dW/dC_a, the lower response slope during
534 the later period suggests that the marginal response of Chinese forests to continuously rising C_a may
535 differ between periods (Norby and Zak 2011). However, the difference in mean dW/dC_a between 2000–
536 2012 and 1961–1999 was not statistically significant ($P = 0.509$); therefore, this between-period
537 difference cannot yet be considered evidence of a long-term decline in dW/dC_a. Long-term C_a enrichment
538 experiments have shown that tree iWUE may vary across periods of progressively increasing C_a,
539 suggesting that physiological regulation under long-term C_a elevation may influence marginal responses
540 (Šantrůček et al. 2025). Previous studies have suggested that such between-period differences may be
541 associated with plant physiological regulation, nutrient supply limitations, and changes in temperature
542 and moisture conditions. However, because this study did not directly measure photosynthetic processes,

biomass changes, or plant nutrient status, these potential mechanisms cannot be directly verified by our results and require further evaluation through long-term controlled experiments and ecosystem observations.

Overall, Chinese forests have exhibited a sustained increase in iWUE over the past half-century; however, within the temporal and sampling ranges examined in this study, we found no statistically significant evidence of a widespread long-term decline in dW/dC_a. Although the mean response slope was relatively lower during the later period, the difference did not reach statistical significance, indicating that the stage-specific variation and its long-term implications remain uncertain and should be evaluated using longer time series and additional observations of ecosystem processes.

4.3 Environmental Associations with Spatial Heterogeneity in dW/dC_a

Although positive C_a-response sensitivity was observed across different regions of China, dW/dC_a varied spatially among the tree-ring $\delta^{13}C$ records (Terrer et al. 2019). We combined partial correlation, Random Forest, and SHAP analyses to examine the relationships of climatic, topographic, and atmospheric CO_2 conditions with spatial variation in dW/dC_a. No individual environmental factor was significantly correlated with dW/dC_a. However, MAP, MAT, and VP ranked relatively high in the Random Forest and SHAP analyses, indicating that hydroclimatic conditions may be associated with spatial variation in forest C_a-response sensitivity.

Water availability strongly influences plant carbon–water exchange (Jiang et al. 2019). In water-limited environments, plants regulate stomatal conductance to balance carbon uptake against water loss, and long-term differences in water availability may therefore influence physiological responses to rising C_a. Previous tree-ring isotope studies have also shown that drought-related conditions can be associated with variation in $\delta^{13}C$ and iWUE, highlighting the relevance of water stress to long-term physiological

565 water-use responses (Hirsch et al. 2023). However, neither AI nor MAP was significantly correlated with
566 dW/dC_a in our analysis, suggesting that a single water-availability metric is insufficient to account for
567 spatial differences in C_a-response sensitivity. These responses are likely shaped by multiple interacting
568 factors, including water availability, atmospheric moisture conditions, and long-term ecological
569 acclimation.

570 Temperature and atmospheric humidity may also influence forest responses to rising C_a (Li et al.
571 2026). Temperature affects photosynthesis, respiration, and carbon balance during the growing season,
572 whereas VP characterizes atmospheric moisture conditions and may influence stomatal regulation and
573 leaf–atmosphere water-vapor gradients (Grossiord et al. 2020). Under high temperatures or drier
574 atmospheric conditions, plants may adjust stomatal conductance, thereby altering the balance between
575 carbon uptake and water loss and potentially affecting iWUE responses to changes in C_a. However, our
576 analysis was based on long-term mean climatic variables rather than growing-season dynamics or
577 indicators of extreme climate events. The relationships between these environmental factors and dW/dC_a
578 therefore require further evaluation.

579 Notably, environmental variables explained substantially less variation in dW/dC_a than in mean
580 iWUE (Lavergne et al. 2019). The Random Forest model yielded an R^2 of −0.17 under leave-one-out
581 cross-validation, indicating limited predictive performance of the available environmental variables at
582 the tree-ring $\delta^{13}C$ sequence level. This may partly reflect the nature of dW/dC_a itself. Whereas iWUE
583 describes the mean carbon–water exchange state over a given period, dW/dC_a is estimated from the
584 relationship between iWUE and C_a and represents a response slope derived from a finite time series. Its
585 estimate may therefore be influenced not only by environmental conditions and plant physiological
586 regulation, but also by record length, temporal coverage, the magnitude of C_a variation, and interannual

environmental variability. Because tree-ring sequences differed in length and temporal coverage, spatial differences in dW/dC_a may reflect both ecological variation and uncertainty in slope estimation. As a response parameter derived from time-series relationships, dW/dC_a is therefore inherently more sensitive to data characteristics than mean-state indicators such as iWUE, which may limit its predictability from environmental variables.

Although MAP, MAT, and VP showed relatively high importance in the Random Forest and SHAP analyses, these results should be interpreted as statistical associations rather than evidence of deterministic environmental controls. Differences in iWUE and its responses to climatic factors among conifer genera in China have also been documented, suggesting that species composition and functional type may contribute to spatial heterogeneity in tree-ring $\delta^{13}C$ records. Given the limited predictive performance of the model, the SHAP results primarily describe the relative contributions of environmental variables to model output within the observed sample range and do not demonstrate that any individual factor determines variation in dW/dC_a. Future studies should incorporate additional ecological and physiological variables, including plant functional traits, stand age, soil moisture, nutrient status, and long-term exposure to extreme climate events, to better resolve the drivers of spatial variation in forest C_a-response sensitivity.

Overall, dW/dC_a varied spatially across Chinese forests, but this variation cannot be attributed to a single climatic gradient. Compared with long-term changes in iWUE, dW/dC_a is a response parameter derived from time-series relationships and is influenced by both ecological conditions and characteristics of the underlying records. Spatial variation in dW/dC_a may therefore reflect a combination of ecological heterogeneity and uncertainty in slope estimation.

4.4 Limitations and Ecological Implications

This study reconstructed changes in forest iWUE in China during 1961–2012 using 34 tree-ring $\delta^{13}C$ records and further examined the temporal and spatial variation in forest C_a-response sensitivity (dW/dC_a). However, several limitations should be considered.

First, owing to the limited spatial availability of publicly accessible tree-ring stable carbon isotope data, the final dataset comprised 34 tree-ring $\delta^{13}C$ records. Although these sequences covered the major climatic regions of China, their spatial distribution remained somewhat uneven. Therefore, our results describe variation in forest iWUE and C_a-response sensitivity across the available sampling sites, but they cannot fully represent long-term changes across all forest types, particularly in some ecologically vulnerable regions and specialized forest ecosystems.

Second, the effective record lengths varied among the tree-ring sequences, which may increase uncertainty in dW/dC_a estimates (Marchand et al. 2020). Because dW/dC_a is estimated from the regression relationship between iWUE and changes in C_a, shorter time series may reduce the ability to identify long-term response trends. In addition, the water-use efficiency reflected by tree-ring $\delta^{13}C$ may vary with season and within-year growth processes, meaning that temporal resolution may also affect the estimation of iWUE and the interpretation of its response relationships. Although this study assessed the robustness of dW/dC_a trends using 5-, 10-, and 20-year moving-window analyses and decadal comparisons, future studies should incorporate longer time series and a larger number of independent tree-ring $\delta^{13}C$ records to further validate regional-scale patterns of forest C_a-response sensitivity.

Third, the iWUE reconstructed from tree-ring $\delta^{13}C$ primarily reflects physiological responses at the tree or leaf scale and cannot directly represent total ecosystem-scale transpiration, carbon assimilation capacity, or water consumption. Therefore, future studies should integrate flux observations, remote-

630 sensing products, and ecosystem models to assess forest carbon–water responses to rising C_a across
631 broader spatial and ecological scales.

632 In addition, the environmental-factor analysis in this study was primarily based on climatic,
633 topographic, and C_a background variables and did not incorporate potentially influential factors such as
634 tree age, plant functional traits, soil properties, nutrient status, and historical disturbances. In particular,
635 tree age, size, and developmental stage may influence water-use efficiency estimated from stable isotopes
636 and its responses to climate and C_a, and these factors may therefore contribute to variation among tree-
637 ring $\delta^{13}C$ records (Brienen et al. 2017). Meanwhile, because of the limited predictive performance of the
638 RF–SHAP analysis, it was used only to explore the relative associations between environmental variables
639 and dW/dC_a and not to infer deterministic causal relationships. Future studies should therefore integrate
640 a broader range of ecological process variables with long-term ecosystem observations and controlled
641 experiments to further elucidate the mechanisms underlying spatial variation in forest C_a-response
642 sensitivity.

643 Despite these limitations, this study provides important insights into the long-term C_a-response
644 processes of forests in China. The results show that forest iWUE in China has generally increased over
645 the past half-century; however, a sustained increase in iWUE does not necessarily imply a synchronous
646 increase in the magnitude of forest responses to rising C_a. As an indicator of the magnitude of iWUE
647 change associated with a unit increase in C_a, dW/dC_a can complement the limitations of conventional
648 analyses focusing solely on long-term iWUE trends. Therefore, when assessing forest ecosystem
649 responses to continuously increasing C_a, focusing only on long-term changes in iWUE may be
650 insufficient; regional differences in C_a-response sensitivity and their potential limiting factors should also
651 be considered.

5 Conclusion

Based on 34 tree-ring $\delta^{13}C$ records from forests across China, we reconstructed long-term variation in forest iWUE during 1961–2012 and assessed temporal trends and spatial variation in forest C_a-response sensitivity (dW/dC_a). Forest iWUE increased significantly over the study period, with all 34 sequences showing positive trends and 33 showing statistically significant increases, indicating a widespread increase in forest iWUE under rising C_a.

Despite the sustained increase in iWUE, dW/dC_a showed no statistically significant long-term decline during 1961–2012, and analyses using multiple temporal windows provided no consistent evidence of a persistent decrease. Although mean dW/dC_a was lower during 2000–2012 than during 1961–1999, the difference between the two periods was not statistically significant ($P = 0.509$). This difference between periods should therefore be evaluated using longer time series.

dW/dC_a varied spatially among forest sequences, but no significant differences were detected among Köppen–Geiger climate regions. Partial correlation, Random Forest, and SHAP analyses indicated that no single climatic or geographic factor adequately explained this spatial variation. MAP, MAT, and VP showed relatively high variable importance, but given the limited predictive performance of the model, these relationships should be interpreted as statistical associations rather than evidence of deterministic environmental controls. Overall, forest iWUE in China increased substantially over the past half-century, whereas dW/dC_a showed no statistically significant long-term decline. The observed spatial variation in dW/dC_a may reflect the combined effects of multiple environmental conditions, plant physiological characteristics, and unmeasured ecological processes.

References

Adams MA, Buckley TN, Turnbull TL (2020) Diminishing CO2-driven gains in water-use efficiency of

674 global forests. Nature Climate Change 10(5):466-471 https://doi.org/10.1038/s41558-020-
675 0747-7
676 Ainsworth EA, Long SP (2005) What have we learned from 15 years of free-air CO2 enrichment (FACE)?
677 A meta-analytic review of the responses of photosynthesis, canopy properties and plant
678 production to rising CO2. New Phytologist 165(2):351-372 https://doi.org/10.1111/j.1469-
679 8137.2004.01224.x
680 Andreu-Hayles L, Planells O, GutiÉRrez E, Muntan E, Helle G, Anchukaitis KJ, Schleser GH (2011)
681 Long tree-ring chronologies reveal 20th century increases in water-use efficiency but no
682 enhancement of tree growth at five Iberian pine forests. Global Change Biology 17(6):2095-
683 2112 https://doi.org/10.1111/j.1365-2486.2010.02373.x
684 Antonucci S, Marshall J, Santopuoli G, Marchetti M, Tognetti R (2023) Tree-ring isotopic composition
685 reveals intraspecific variation in water use efficiency of Pinus pinaster Ait. provenances grown
686 in common gardens. Trees 37(6):1767-1780 https://doi.org/10.1007/s00468-023-02458-6
687 Bates D, Mächler M, Bolker B, Walker S (2015) Fitting Linear Mixed-Effects Models Using lme4.
688 Journal of Statistical Software 67(1):1-48 https://doi.org/10.18637/jss.v067.i01
689 Battipaglia G, Saurer M, Cherubini P, Calfapietra C, McCarthy HR, Norby RJ, Francesca Cotrufo M
690 (2013) Elevated CO2 increases tree-level intrinsic water use efficiency: insights from carbon
691 and oxygen isotope analyses in tree rings across three forest FACE sites. New Phytologist
692 197(2):544-554 https://doi.org/10.1111/nph.12044
693 Beck HE, Zimmermann NE, McVicar TR, Vergopolan N, Berg A, Wood EF (2018) Present and future
694 Köppen-Geiger climate classification maps at 1-km resolution. Scientific Data 5(1):180214
695 https://doi.org/10.1038/sdata.2018.214

Breiman L (2001) Random Forests. Machine Learning 45(1):5-32 https://doi.org/10.1023/A:1010933404324

Brienen RJW, Gloor E, Clerici S, Newton R, Arppe L, Boom A, Bottrell S, Callaghan M, Heaton T, Helama S, Helle G, Leng MJ, Mielikäinen K, Oinonen M, Timonen M (2017) Tree height strongly affects estimates of water-use efficiency responses to climate and CO(2) using isotopes. Nat Commun 8(1):288 https://doi.org/10.1038/s41467-017-00225-z

Brienen RJW, Wanek W, Hietz P (2011) Stable carbon isotopes in tree rings indicate improved water use efficiency and drought responses of a tropical dry forest tree species. Trees 25(1):103-113 https://doi.org/10.1007/s00468-010-0474-1

Ding Y, Wen L, Zhang J, Zhang W, Chen H, Song S, Lai Z, Zhou J, Lin G (2026) Long-term increases in tree water-use efficiency across China are associated with CO2 and hydroclimatic variation. Journal of Hydrology 679:136114 https://doi.org/10.1016/j.jhydrol.2026.136114

Farquhar GD, Ehleringer JR, Hubick KT (1989) Carbon Isotope Discrimination and Photosynthesis. Annual Review of Plant Physiology and Plant Molecular Biology 40:503-537 https://doi.org/10.1146/annurev.pp.40.060189.002443

Farr TG, Rosen PA, Caro E, Crippen R, Duren R, Hensley S, Kobrick M, Paller M, Rodriguez E, Roth L, Seal D, Shaffer S, Shimada J, Umland J, Werner M, Oskin M, Burbank D, Alsdorf D (2007) The Shuttle Radar Topography Mission. Reviews of Geophysics 45(2):RG2004 https://doi.org/10.1029/2005RG000183

Franks PJ, Adams MA, Amthor JS, Barbour MM, Berry JA, Ellsworth DS, Farquhar GD, Ghannoum O, Lloyd J, McDowell N, Norby RJ, Tissue DT, von Caemmerer S (2013) Sensitivity of plants to changing atmospheric CO2 concentration: from the geological past to the next century. New

718 Phytol 197(4):1077-1094 https://doi.org/10.1111/nph.12104
719 Fu L, Xu Y, Xu Z, Wu B, Zhao D (2020) Tree water-use efficiency and growth dynamics in response to
720 climatic and environmental changes in a temperate forest in Beijing, China. Environment
721 International 134:105209 https://doi.org/10.1016/j.envint.2019.105209
722 Gebrekirstos A, van Noordwijk M, Neufeldt H, Mitlöhner R (2011) Relationships of stable carbon
723 isotopes, plant water potential and growth: an approach to asses water use efficiency and growth
724 strategies of dry land agroforestry species. Trees 25(1):95-102 https://doi.org/10.1007/s00468-
725 010-0467-0
726 Gentilesca T, Battipaglia G, Borghetti M, Colangelo M, Altieri S, Ferrara AMS, Lapolla A, Rita A,
727 Ripullone F (2021) Evaluating growth and intrinsic water-use efficiency in hardwood and
728 conifer mixed plantations. Trees 35(4):1329-1340 https://doi.org/10.1007/s00468-021-02120-z
729 Grossiord C, Buckley TN, Cernusak LA, Novick KA, Poulter B, Siegwolf RTW, Sperry JS, McDowell
730 NG (2020) Plant responses to rising vapor pressure deficit. New Phytol 226(6):1550-1566
731 https://doi.org/10.1111/nph.16485
732 Guerrieri R, Belmecheri S, Ollinger SV, Asbjornsen H, Jennings K, Xiao J, Stocker BD, Martin M,
733 Hollinger DY, Bracho-Garrillo R, Clark K, Dore S, Kolb T, Munger JW, Novick K, Richardson
734 AD (2019) Disentangling the role of photosynthesis and stomatal conductance on rising forest
735 water-use efficiency. Proc Natl Acad Sci U S A 116(34):16909-16914
736 https://doi.org/10.1073/pnas.1905912116
737 Han Y, Li S, Wang J, Guo Y, Fan R, Zhang H, Liu Q, Zhao Y (2023) Responses of Picea meyeri to
738 Climatic Factors Revealed by Tree Ring Isotopes and Water Use Efficiency on Luya Mountain
739 of North-Central China. Atmosphere 14:615 https://doi.org/10.3390/atmos14040615

Hirsch M, Böddeker H, Albrecht A, Saha S (2023) Drought tolerance differs between urban tree species but is not affected by the intensity of traffic pollution. Trees 37(1):111-131 https://doi.org/10.1007/s00468-022-02294-0

Jiang Y, Still CJ, Rastogi B, Page GFM, Wharton S, Meinzer FC, Voelker S, Kim JB (2019) Trends and controls on water-use efficiency of an old-growth coniferous forest in the Pacific Northwest. Environmental Research Letters 14(7):074029 https://doi.org/10.1088/1748-9326/ab2612

Keenan TF, Hollinger DY, Bohrer G, Dragoni D, Munger JW, Schmid HP, Richardson AD (2013) Increase in forest water-use efficiency as atmospheric carbon dioxide concentrations rise. Nature 499(7458):324-327 https://doi.org/10.1038/nature12291

Knauer J, Zaehle S, Reichstein M, Medlyn BE, Forkel M, Hagemann S, Werner C (2017) The response of ecosystem water-use efficiency to rising atmospheric CO2 concentrations: sensitivity and large-scale biogeochemical implications. New Phytologist 213(4):1654-1666 https://doi.org/10.1111/nph.14288

Lavergne A, Graven H, De Kauwe MG, Keenan TF, Medlyn BE, Prentice IC (2019) Observed and modelled historical trends in the water-use efficiency of plants and ecosystems. Global Change Biology 25(7):2242-2257 https://doi.org/10.1111/gcb.14634

Li D, Fang K, Li Y, Chen D, Liu X, Dong Z, Zhou F, Guo G, Shi F, Xu C, Li Y (2017) Climate, intrinsic water-use efficiency and tree growth over the past 150 years in humid subtropical China. PLOS ONE 12(2):e0172045 https://doi.org/10.1371/journal.pone.0172045

Li Y, Wang Y, Xu W, Tan J (2026) Rising atmospheric CO2 outweighs elevated vapor pressure deficit in explaining increased intrinsic water use efficiency in Chinese pine. Frontiers in Plant Science 17:1721057 https://doi.org/10.3389/fpls.2026.1721057

762 Mann HB (1945) Nonparametric Tests Against Trend. Econometrica 13(3):245-259
763 https://doi.org/10.2307/1907187
764 Marchand W, Girardin MP, Hartmann H, Depardieu C, Isabel N, Gauthier S, Boucher É, Bergeron Y
765 (2020) Strong overestimation of water-use efficiency responses to rising CO2 in tree-ring
766 studies. Global Change Biology 26(8):4538-4558 https://doi.org/10.1111/gcb.15166
767 Mathias JM, Thomas RB (2021) Global tree intrinsic water use efficiency is enhanced by increased
768 atmospheric CO(2) and modulated by climate and plant functional types. Proc Natl Acad Sci U
769 S A 118(7):e2014286118 https://doi.org/10.1073/pnas.2014286118
770 McCarroll D, Loader NJ (2004) Stable isotopes in tree rings. Quaternary Science Reviews 23(7):771-
771 801 https://doi.org/10.1016/j.quascirev.2003.06.017
772 Medrano H, Flexas J, Galmés J (2009) Variability in water use efficiency at the leaf level among
773 Mediterranean plants with different growth forms. Plant and Soil 317(1):17-29
774 https://doi.org/10.1007/s11104-008-9785-z
775 Norby R, Zak D (2011) Ecological Lessons from Free-Air CO2 Enrichment (FACE) Experiments.
776 Annual Review of Ecology, Evolution, and Systematics 42:181-203
777 https://doi.org/10.1146/annurev-ecolsys-102209-144647
778 Pan Y, Birdsey RA, Fang J, Houghton R, Kauppi PE, Kurz WA, Phillips OL, Shvidenko A, Lewis SL,
779 Canadell JG, Ciais P, Jackson RB, Pacala SW, McGuire AD, Piao S, Rautiainen A, Sitch S,
780 Hayes D (2011) A Large and Persistent Carbon Sink in the World's Forests. Science
781 333(6045):988-993 https://doi.org/10.1126/science.1201609
782 Peñuelas J, Canadell JG, Ogaya R (2011) Increased water-use efficiency during the 20th century did not
783 translate into enhanced tree growth. Global Ecology and Biogeography 20(4):597-608

784 https://doi.org/10.1111/j.1466-8238.2010.00608.x
785 Pons TL, Helle G (2011) Identification of anatomically non-distinct annual rings in tropical trees using
786 stable isotopes. Trees 25(1):83-93 https://doi.org/10.1007/s00468-010-0527-5
787 Rozendaal DMA, Zuidema PA (2011) Dendroecology in the tropics: a review. Trees 25(1):3-16
788 https://doi.org/10.1007/s00468-010-0480-3
789 Šantrůček J, Kubásek J, Janová J, Šantrůč KH, Altman J, Tumajer J, Hrádková M, Cienciala E (2025)
790 Response of leaf internal CO(2) concentration and intrinsic water-use efficiency in Norway
791 spruce to century-long gradual CO(2) elevation. Photosynthetica 63(1):51-63
792 https://doi.org/10.32615/ps.2025.006
793 Saurer M, Siegwolf RTW, Schweingruber FH (2004) Carbon isotope discrimination indicates improving
794 water-use efficiency of trees in northern Eurasia over the last 100 years. Global Change Biology
795 10(12):2109-2120 https://doi.org/10.1111/j.1365-2486.2004.00869.x
796 Stone M (1974) Cross-Validatory Choice and Assessment of Statistical Predictions. Journal of the Royal
797 Statistical Society: Series B (Methodological) 36(2):111-133 https://doi.org/10.1111/j.2517-
798 6161.1974.tb00994.x
799 Terrer C, Jackson RB, Prentice IC, Keenan TF, Kaiser C, Vicca S, Fisher JB, Reich PB, Stocker BD,
800 Hungate BA, Peñuelas J, McCallum I, Soudzilovskaia NA, Cernusak LA, Talhelm AF, Van
801 Sundert K, Piao S, Newton PCD, Hovenden MJ, Blumenthal DM, Liu YY, Müller C, Winter K,
802 Field CB, Viechtbauer W, Van Lissa CJ, Hoosbeek MR, Watanabe M, Koike T, Leshyk VO,
803 Polley HW, Franklin O (2019) Nitrogen and phosphorus constrain the CO2 fertilization of
804 global plant biomass. Nature Climate Change 9(9):684-689 https://doi.org/10.1038/s41558-
805 019-0545-2

Wang W, Liu X, An W, Xu G, Zeng X (2012) Increased intrinsic water-use efficiency during a period with persistent decreased tree radial growth in northwestern China: Causes and implications. Forest Ecology and Management 275:14-22 https://doi.org/10.1016/j.foreco.2012.02.027

Zhang Z, Zhang L, Xu H, Creed IF, Blanco JA, Wei X, Sun G, Asbjornsen H, Bishop K (2023) Forest water-use efficiency: Effects of climate change and management on the coupling of carbon and water processes. Forest Ecology and Management 534:120853 https://doi.org/10.1016/j.foreco.2023.120853

Zomer RJ, Xu J, Trabucco A (2022) Version 3 of the Global Aridity Index and Potential Evapotranspiration Database. Sci Data 9(1):409 https://doi.org/10.1038/s41597-022-01493-1

Statements and Declarations

Funding

This work was supported by the National Undergraduate Innovation and Entrepreneurship Training Program (Grant No. X2026141600001) and the Post-doctoral Later-stage Foundation Project of Shenzhen Polytechnic University (Grant No. 6023271029K).

Author Contributions

K.Y. Hong and Y.X. Xia contributed equally to this work. K.Y. Hong was responsible for conceptualization, methodology, software, data curation, formal analysis, visualization, and writing the original draft. Y.X. Xia contributed to conceptualization, methodology, data processing, statistical analysis, visualization, and manuscript revision. M.Y. Li contributed to conceptualization, resources, project administration, funding acquisition, supervision, and review and editing of the manuscript. F. Yue contributed to validation, methodological discussion, and manuscript revision. Z.L. Sun contributed to validation and review of the manuscript. L.D. Zou contributed to data validation, methodological

discussion, and manuscript review.

All authors have read and agreed to the published version of the manuscript.

Competing interests

The authors declare that they have no competing interests.

Data Availability

The tree-ring $\delta^{13}C$ data used in this study were obtained from the global tree-ring stable carbon isotope dataset compiled by Adams et al. (2020), which is publicly available through the Zenodo data repository (https://doi.org/10.5281/zenodo.3693240). Based on the geographic coordinates of the tree-ring records and the national boundaries of China, we selected the $\delta^{13}C$ records located within China from this global dataset. Climate data were obtained from the CRU TS v4.09 global climate dataset (https://crudata.uea.ac.uk/cru/data/hrg/cru_ts_4.09/cruts.2503051245.v4.09/). Elevation data were obtained from the NASA Shuttle Radar Topography Mission (SRTM) digital elevation model through the Google Earth Engine (GEE) platform. Köppen–Geiger climate classification data were obtained from the global climate classification dataset published by Beck et al. (2018) (https://doi.org/10.6084/m9.figshare.6396959). All datasets used in this study are publicly available.

Code Availability

The analysis code used in this study will be archived on Zenodo and made publicly available upon publication of the manuscript.

Supplementary Files

This is a list of supplementary files associated with this preprint. Click to download.

- OnlineResource1.docx